26 Role of Intermediate Species in Controlling Ignition Timing of HCCI

(1) (1) (1) (2) (1)
Mitsuaki OHTOMO, Takehiro YAMAGUCHI, Masataka YOSHII, Hiroyuki YAMADA, Atsumu TEZAKI

(1) School of Engineering, The University of Tokyo, Bunkyo, Hongo, Tokyo 113-8656 Japan

(2) National Traffic Safety and Environment Laboratory, Jindaijihigashimachi, Chofu, Tokyo 182-0012 Japan

The chemical mechanism responsible for controlling ignition timing by using additives in HCCI has been investigated. Dimethyl ether (DME) and methanol were used as the main fuel and the additive, respectively. Fuel consumption and intermediate formation in the first stage (cool ignition) were measured with crank angle resolved pulse-valve sampling and exhaust gas analysis, where HCHO, HCOOH, CO, H_2O_2 and other species were detected as the intermediate. The effect of methanol addition retarding ignition is represented by an analytical model in which the growth rate of the chain reaction is reduced by the methanol addition.

***Keywords*: Ignition, Combustion, Chemical Analysis, Control, Additive/HCCI, Chemical Mechanism**

1. INTRODUCTION

A typical process of premixed compression ignition consists of two distinct stages of heat release. The first stage (cool ignition) is incomplete oxidation whose extent is considerably dependent on the fuel property such as octane number, whereas the latter stage (hot ignition) is total oxidation with the mechanism common to most hydrocarbons[1]. Ignition timings can be controlled by using additives enhancing or depressing the activity of the cool ignition[2-5], where the combined effect of the additive and intermediate products influences the low temperature oxidation mechanism. In this regard, monitoring the formation of intermediate species during ignition is useful to validate the chemical mechanistic models and guide to better control HCCI.

As a method of the transient species detection, crank angle resolved in-cylinder sampling was conducted in dimethyl ether (DME) fueled HCCI[6] and in butane based HCCI[7]. By means of an electrically driven pulse valve equipped onto the cylinder, species like HCHO and CH_4 were recognized to be present between the stages of ignition; however, only qualitative correspondence with model calculations was obtained. Probably insufficient time resolution of the sampling and storage in sampling vessels caused significant errors. Typical valve open duration in the former studies is 1.5 ms, which is equivalent to 5 – 9 CA at 600 – 1000 RPM engine operation. This period is necessary for sufficient amount of sampling from the reacting volume in the cylinder over that from quenched volume near wall and in tubing.

Our previous work employed another approach; namely, exhaust gas analysis was conducted in the condition of hot ignition suppressed, single cool ignition[8]. Through the observation that formaldehyde/ DME ratio after cool ignitions is constant within a range of equivalence ratio, the role of formaldehyde terminating the OH reproducing chain reaction system was elucidated. The same methodology was applied to a system controlling ignition timing by adding methanol and ozone[5]. These experimental observations were reasonably reproduced by simulations using detailed chemical kinetic models of DME oxidation. However, the effective range of equivalence ratio applicable by this method alone is limited.

In this work, we employ an improved device for time resolved sampling measurement of in-cylinder species composition and apply it to DME fueled HCCI. As well, exhaust gas analysis with a Fourier transform IR spectrometer (FT-IR) is conducted to obtain further information of the intermediate behaviors in ignition. In particular, methanol is used as an ignition suppressing additive and the chemical mechanism causing the effect is discussed in comparison with simulations using existing models of detailed DME oxidation mechanism[9, 10].

2. EXPERIMENTAL SETUP

2.1 MOTORED ENGINE

The base engine is a 4-stroke, side valve single cylinder type of bore × stroke = 84 × 70 [mm]. The compression ratio after modification is 8.0. The engine

crank is externally driven by a 1500 W induction motor in order to rotate at a constant speed regardless of internal power generation. The standard speed was set at 600 RPM. DME is supplied from a commercial cylinder, regulated through a 2 SLPM mass flow controller, and mixed with air at the intake. The air is aspirated through a mass flow meter and a surge tank, and preheated to around 400 K to meet the ignition condition at the current compression ratio. The engine head is also heated so that the mounted thermocouple equipped on engine head indicates the same temperature as the intake temperature during the steady state operation. The engine head was replaced to equip a pressure pickup and a pulse sampling system described in the next subsection.

2.2 PULSE SAMPLING

The engine system equipped with a sampling system is schematically shown in Fig. 1. A solenoid-type pulse valve (General Valve, 0.8 mm orifice diameter) is screwed on the head plate of the engine. The outlet of the valve is directly connected to a vacuum chamber continuously pumped by a mechanical booster pump. The chamber has an orifice connected to a high vacuum chamber, in which a QMS detector (Anelva, M-400GA-DTS) is installed, pumped by a turbo-molecular pump. The orifice size of 1 mm was used in the current experiments.

In this setup, the direct QMS detection in the differential pumping system allows to set the valve open duration less than 0.5 ms with sufficient sensitivity, while 0.3 ms of the mechanical delay to actual open is present. However, simple sampling with short duration causes erroneous outcomes. As demonstrated in Fig.2, unburned DME is dominant in the sampling from DME-air compression cycles with valve open duration shorter than 0.5 ms, even though it is sampled at 60 deg ATDC, i.e., after complete combustion. On the other hand, CO_2 becomes dominant at longer sampling duration. This fact indicates that the valve at first samples out unreacted volume such as in dead volume of the valve and in boundary layer on the wall before extracting the reacted core volume.

According to the above observation, a correction scheme is established so as to extract the core volume signals as:

$$\text{Corrected signal} = S(\mathrm{X}: t_b)/S(\mathrm{N_2}: t_b) - S(\mathrm{X}: t_a)/S(\mathrm{N_2}: t_a),$$

where S is the raw QMS signal, X is the detecting species, and t_a and t_b are two different sampling durations. When t_a was set at 0.6 ms and t_b was varied over 0.7 and 1.0 ms, the corrected signals were confirmed to be constant. Finally we set t_a and t_b as 0.6 - 0.7ms and 1.2 - 1.3ms, respectively, considering the trade-off between S/N ratio and time resolution. The sampling amount at 1 ms of open duration was estimated to be 0.06 cm^3 as a volume at the in-cylinder pressure.

DME (mass-charge ratio m/e = 46), HCHO (30), H_2O_2 (34), CO_2 (44) and H_2O (18) are measured in this method of CA resolved sampling. N_2 (28) is monitored as the standard signal representing total sampled amount. In the QMS setting, the electron impact ionization energy is set at 20 eV for species except H_2O_2. This is lower than the normal ionization energy of 70 eV, but the undesirable fragmentation is avoided without losing sensitivity. For H_2O_2, higher energy of 45 eV is applied to compensate the weak signals. It was confirmed that no fragment ion was detected at m/e = 34 from standard samples of heavier mass including the above species, HCOOH and $HCOOCH_3$.

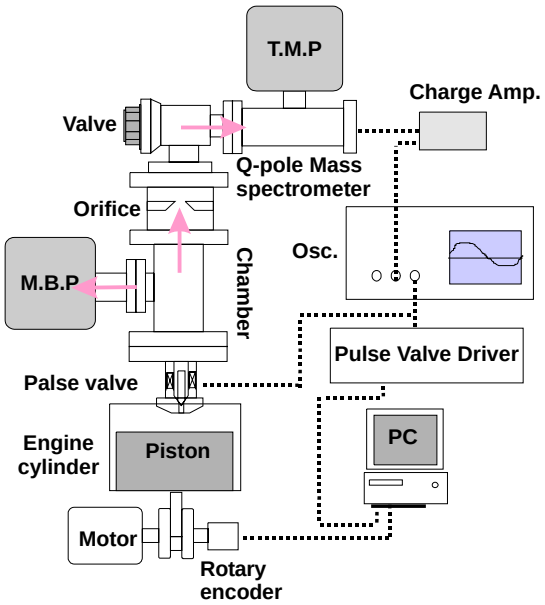

Fig. 1 Schematic of pulse sampling engine system.

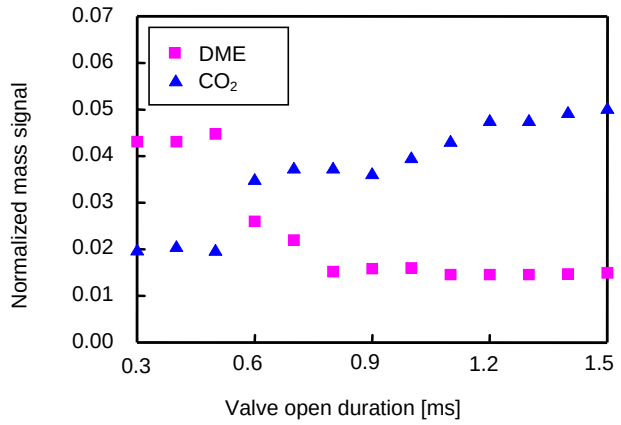

Fig. 2 Mass signals sampled through the pulse valve and normalized by N_2 signal, as a function of valve open duration in the compression of DME-air mixture at fixed CA of 60° ATDC. Equivalence ratio = 0.39 and intake temperature = 414 K

2.3 EXHAUST GAS ANALYSIS

A Fourier transform IR spectrometer (FTIR: IR Prestige-21 from Shimadzu) is used as a detector in this study. A portion of exhaust gas is fed into a 10 cm single path IR cell or a 3 m multi-path cell mounted in the spectrometer. The 10 cm cell is heated to 323 K to avoid water condensation in the cell filled with the exhaust gas at atmospheric pressure. In the case of 3 m cell, exhaust gas is filled at 10 kPa and used without heating. Tubing between exhaust port and the cell is also heated above 323 K. Usually an IR spectrum is obtained as an average of 30 scans with a resolution of 0.5 cm^{-1}.

DME, HCHO, HCOOH, CO and CO_2 are detected with sufficient sensitivity and selectivity in exhaust of DME-air compression in which a single cool ignition is established at equivalence ratio over 0.1. Their mole fractions are calibrated using standard samples. Usually a standard sample contains 0.2 % of the calibrating species. $HCOOCH_3$ and HCHO are also identified. However, notable peaks in the IR range are limited and are superimposed by other spectrum, consequently the quantitative accuracy is marginal.

3. RESULTS AND ANALYSIS

3.1 CRANK ANGLE RESOLVED SAMPLING

Figures 3 and 4 show profiles of species fractions obtained by the current sampling method together with pressure and rate of heat release (ROHR). On the species profiles, calibrations using standard gas of known concentration were conducted for DME, HCHO and H_2O_2, so that they are expressed in mole fractions. For CO_2 and H_2O, QMS signals normalized by that of N_2 are indicated. At lower equivalence ratio of 0.25 shown in Fig. 5, the single peak of ROHR corresponds to cool ignition while hot ignition is suppressed. Consumption of DME and formation of intermediates begin at a close timing to the onset of the heat release. The species fractions change only gradually after the end of the cool ignition heat release. It is convincingly that the observed final composition conserves in the expansion period until the exhaust valve to open. At higher equivalence ratio of 0.36, the two-stage ignition of distinct cool and hot stages appeared as shown in Fig. 4. The high pressure of the hot ignition is beyond the level that the pulse valve stably operates; therefore sampling was not conducted between -20 and 30 ATDC. It is recognized that the fuel DME is partly consumed at the cool ignition and totally consumed at the hot ignition. On the other hand, the intermediate, HCHO and H_2O_2 are produced at the cool ignition and consumed at the hot ignition. Amounts of CO_2 and H_2O after the cool ignition are small fractions of the final ones after the hot ignition. The small deviations in the timing between heat release and species profiles are probably due to the difference in the nature that ROHR is volume averaged and the sampling is from a point of the volume; although timing shift during a course of experiment may be partly responsible. It is noted that the specific time of the species concentration change is shorter than that of ROHR, which demonstrates the good resolution of the current sampling method.

The detection of H_2O_2 is a notable result of the direct *in vacuo* detection. Although the importance of H_2O_2 as a triggering agent for hot ignition has been pointed out in many modeling studies, the unstable and low vapor pressure species was not detected in former sampling studies with storage bags.

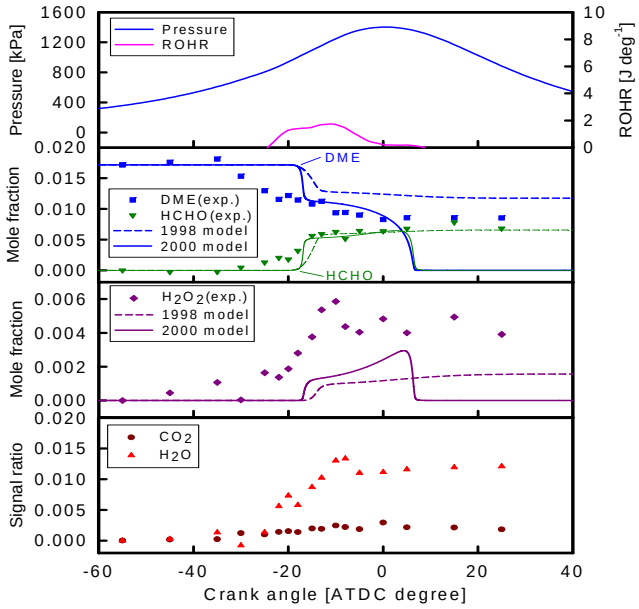

Fig. 3 Crank angle resolved profiles of pressure and heat release rate and species mole fractions. Equivalence ratio = 0.25, intake temperature = 410 K.

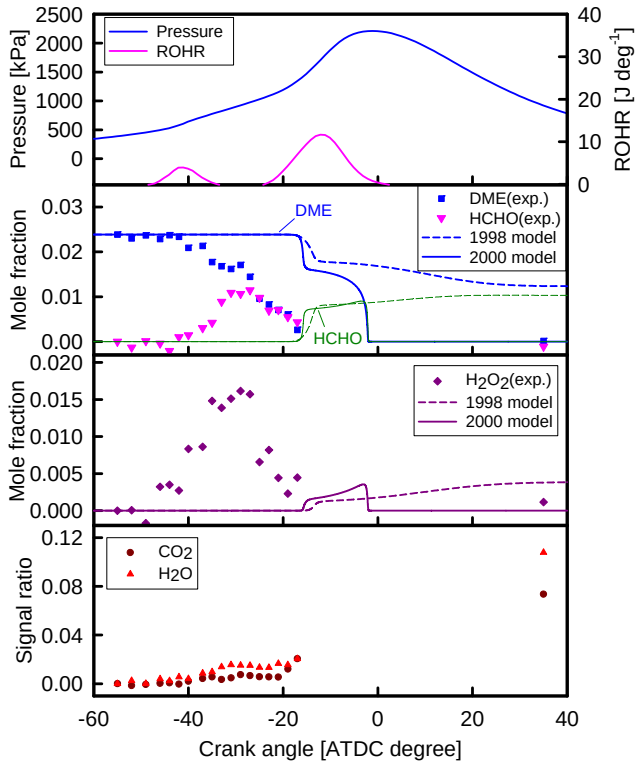

Fig. 4 Crank angle resolve profiles at equivalence ratio = 0.36.

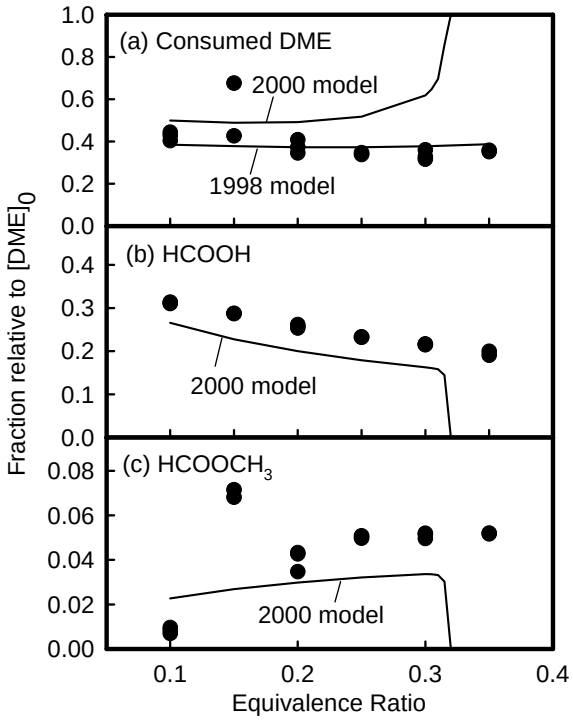

Fig. 5 (a) DME consumption, (b) HCOOH and (c) $HCOOCH_3$ formation relative to initial amount of DME as a function of equivalence ratio. Intake temperature = 373 K.

3.2 EXHAUST GAS ANALYSIS OF COOL IGNITION

Figure 5 shows DME consumption and product emissions at the exhaust as a function of equivalence ratio. Vertical scales are normalized by that of initial DME fraction. In experiment and the model 1998, single cool ignition condition is maintained throughout the range of equivalence ratio. The percentage DME consumption is a very weak function of equivalence ratio lying around 40 %. In contrast, hot ignition occurs at equivalence ratio over 0.3 in model 2000, so that the fuel and intermediates are totally consumed in this region. HCOOH yield shows a decreasing trend with increasing equivalence ratio, whereas $HCOOCH_3$ yield shows opposite, increasing trend. These trends of intermediates that are not included in the model 1998 are reproduced by the model 2000 within the range of single cool ignition.

3.3 EFFECT OF METHANOL ADDITION

Methanol was added in the compression of DME-air mixture and the exhaust was analyzed by FT-IR in the 3 m cell. Figure 6 compares the measured species mole fractions with those simulated. DME fraction increases with increasing methanol addition towards the level of no consumption, whereas HCOOH and CO fractions decrease with methanol addition. The DME and CO results over the range of methanol addition are well reproduced by the model 1998, although only the model

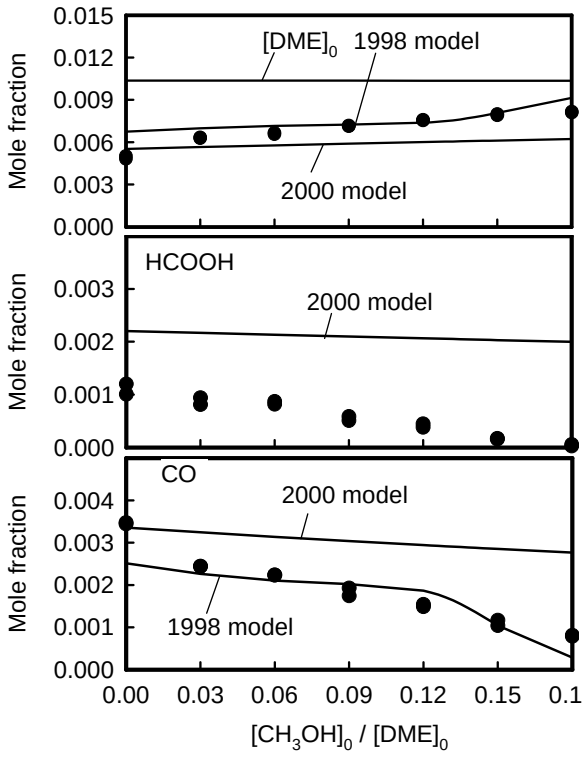

Fig. 6 Effect of methanol addition in species mole fractions in exhaust of DME-air compression. DME equivalence ratio = 0.15, intake temperature = 383 K.

shows change of slope at 12 % addition. In contrast, the methanol effect is considerably less in the model 2000. In the case of HCOOH, only the model 2000 represents the formation, though, the model still underestimates the methanol effect reducing the HCOOH formation.

The above observation of species formation is in coincidence with that of heat release as shown in Fig. 7. It is recognized that fuel consumption, intermediate formation and heat release are generally in proportion. Although both models exhibit the decreasing trend of cool ignition with methanol addition, the experimentally observed reducing heat release almost disappearing at 20 % methanol addition is considerably underestimated by the models.

3.4 LOW TEMPERATURE OXIDATION MECHANISM OF DME

In our former paper[8], we proposed a simplified formulation for the cool ignition of DME compression by extracting essential reaction processes from the detailed model 1998 and it was successful to represent the extent of partial oxidation in a range of equivalence ratio. Here we modify the former formulation to adapt the model

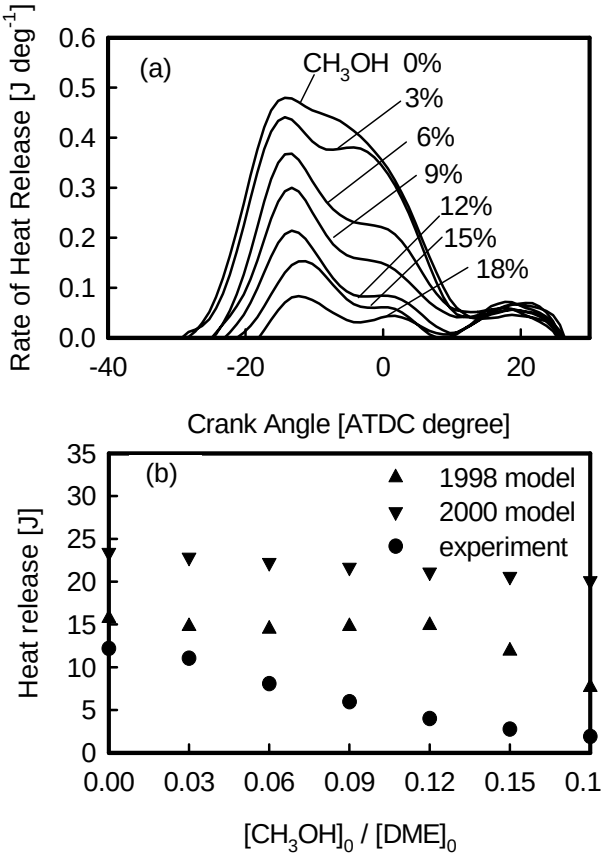

Fig. 7 (a) Measured profiles of cool ignition heat release at various addition of methanol to DME. DME equivalence ratio = 0.15, intake temperature = 383 K. (b) Total heat release of cool ignitions as a function of methanol addition.

2000 mechanism and the effect of methanol addition.

Among the newly confirmed intermediates, $HCOOCH_3$ is a small yield secondary product and negligible in the overall kinetics, but HCOOH is a significant product in low-temperature oxidation comparable to HCHO and should be properly treated.

The essential chemical kinetics of DME oxidation in the cool ignition regime is described as below:

DME + OH → αOH + βHCHO + γHCOOH + other products (R-1)

HCHO + OH → εHCOOH + other products (R-2)

HCOOH + OH → ηOH + other products (R-3)

The chain reaction sequence is summarized in (R-1), where the OH reproduction index α larger than unity assures the growth of the system initially. When the intermediates are formed in considerable concentration, they also react with OH to modify the OH reproduction coefficient. Differential equations for concentrations of OH and relevant species are derived from the kinetic relationship in the above reactions. A set of equations of time independent format is as below:

$$\frac{dy}{dq} = \beta - \frac{k_2}{k_1}\frac{y}{1-q} \qquad \frac{dz}{dq} = \gamma + \varepsilon\frac{k_2}{k_1}\frac{y}{1-q} - \frac{k_3}{k_1}\frac{z}{1-q}$$

where k_i is the rate constant of i th reaction,

$$q = \frac{[\mathrm{DME}]_0 - [\mathrm{DME}]}{[\mathrm{DME}]_0} \quad y = \frac{[\mathrm{HCHO}]}{[\mathrm{DME}]_0} \quad z = \frac{[\mathrm{HCOOH}]}{[\mathrm{DME}]_0}$$

and $[\mathrm{DME}]_0$ is the initial concentration of DME. The growth of chain carrier OH is given as:

$$\frac{d[\mathrm{OH}]}{dt} = \{(\alpha-1)k_1[\mathrm{DME}] - k_2[\mathrm{HCHO}] + (\eta-1)k_3[\mathrm{HCOOH}]\}[\mathrm{OH}] = g[\mathrm{OH}]$$

The chain system terminates when the factor g falls down to zero, thus the end of cool ignition is determined. Integrating y and z deriving g along q until g = 0 gives the extent of fuel consumption and product yields in a cool ignition, where kinetic parameters can be extracted from a detailed reaction mechanism.

In the case of methanol addition, the reaction of methanol with OH should be included:

$CH_3OH + OH \rightarrow HCHO$ + other products (R-4)

so that the y and g equations are modified as:

$$\frac{dy}{dq} = \beta - \frac{k_2}{k_1}\frac{y}{1-q} + \frac{k_2}{k_1}w(1-q)^{(k4/k1-1)}$$

$$g = (\alpha-1)k_1[\mathrm{DME}] - k_2[\mathrm{HCHO}] + (\eta-1)k_3[\mathrm{HCOOH}] - k_4[\mathrm{CH_3OH}]$$

where $w = [CH_3OH]_0/[DME]_0$ and

$$\frac{d[CH_3OH]}{d[DME]} = \frac{k_4[CH_3OH]}{k_1[DME]}$$

Figure 8 shows calculated results of the cool ignition fuel consumption as a function of methanol addition. In the comparison of detailed and the simplified formulation with original parameters extracted from the detailed model shows basically good agreement except of the small discrepancy of the methanol dependence and the abrupt slope change in the detailed model 1998 at 13 % of methanol addition. With the original set of parameters, the model 2000 tends to overestimate the DME consumption whereas the model 1998 shows the opposite trend. Both models underestimate the dependence on methanol addition.

It was found the DME consumption is sensitive to the OH reproduction index α. Modification of α from the original value of 1.52 to 1.80 in the case of the model 1998, and 1.82 to 1.60 in the case of the model 2000 exhibit better agreement with experimentally observed, as also shown in Fig. 8. However, the slope against the methanol addition is not changed by the α modification.

4. CONCLUSIONS

Two methodologies of Intermediate species detection have been applied to premixed compression ignition of dimethyl ether in a motored engine. The results are summarized as:

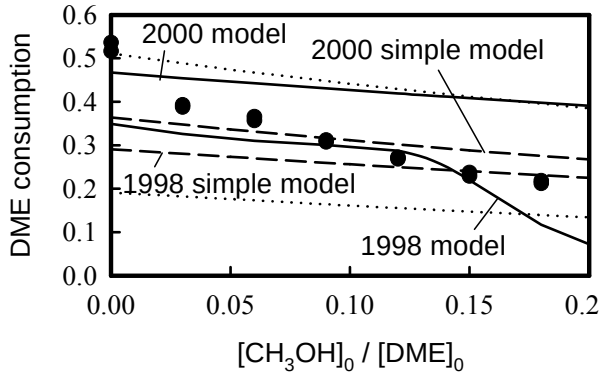

Fig. 8 Fuel consumption at cool ignitions dependent on methanol addition calculated by detailed and simplified models. Solid lines are detailed models, dotted lines are simplified models without parameter modification and dashed lines are simplified models with modification of α. (see text)

The direct mass-spectrometric detection without sample storage enabled detection of unstable hydrogen peroxide appearing in the short period between cool and hot ignitions. By a correction extracting signals of reactive core volume in the cylinder using samples of different valve open durations, effective resolution of 2 CA has been achieved.

Detection of HCOOH and $HCOOCH_3$ in the exhaust gas analysis for cool ignition composition using IR spectrometer has validated the advantage in the newer version of Curran et al. DME oxidation model, while the issue of the version overestimating the extent of cool ignition is indicated.

The essential part of the mechanism determining partial oxidation of cool ignition can be approximated as a chain reaction system yielding certain amounts of OH, HCHO and HCOOH, in which HCHO acts as a major agent for the chain termination. The effect of methanol addition is also included in the scheme to represent the ignition depressing property caused by the OH consumption in the low temperature chain reaction system.

ACKNOWLEDGMENTS

This work was financially supported by a Grant-in-Aid for Scientific Research (B), 1536106, 2003 from the Ministry of Education, Science, Sports and Culture (MEXT).

REFERENCES

1. Westbrook, C. K., Proc. Combust. Inst. 28: 1563 (2000).
2. Ogawa, H., Kaneko, N., Ando, H. and Miyamoto, N., SAE Paper, 2003-01-0746.
3. Tanaka, S., Ayala, F., Keck, J. C. and Heywood, J. B., Combust. Flame, 132: 219 (2003).
4. Aceves, S. M., Flowers, D., Martinez-Frias, J., Espinosa-Loza, F., Pitz, W. J. and Dibble, R., SAE Paper 2003-01-1814.
5. Yamada, H., Yoshii, M., and Tezaki, A., Proc. Combust. Inst. 30: 2773 (2005).
6. Konno, M., and Chen, Z., SAE paper 2003-01-1826 (2003).
7. Furutani, M., Isogai, T., and Ohta, Y, SAE paper 2003-01-1857 (2003).
8. Yamada, H., Suzaki, K., Sakanashi, H., Choi, N., and Tezaki, A., Combust. Flame 140: 24 (2005).
9. Curran, H. J., Pitz, W. J., Westbrook, C. K., Dagaut, P., Boettner, J-C., and Cathonnet, M., Int. J. Chem. Kinet., 30: 229 (1998).
10. Curran, H. J., Fischer, S. L., and Dryer, F. L., Int. J. Chem. Kinet., 32: 741 (2000).